

Research Article

1,4-Dihydropyridine Calcium Channel Blockers: Homology Modeling of the Receptor and Assessment of Structure Activity Relationship

Moataz A. Shaldam, Mervat H. Elhamamsy, Eman A. Esmat, and Tarek F. El-Moselhy

Department of Pharmaceutical Chemistry, Faculty of Pharmacy, Tanta University, Tanta 31527, Egypt

Correspondence should be addressed to Tarek F. El-Moselhy; telmoselhy@yahoo.com

Received 28 September 2013; Accepted 5 December 2013; Published 10 February 2014

Academic Editors: R. B. de Alencastro, P. L. Kotian, O. A. Santos-Filho, L. Soulère, and S. Srichairatanakool

Copyright © 2014 Moataz A. Shaldam et al. This is an open access article distributed under the Creative Commons Attribution License, which permits unrestricted use, distribution, and reproduction in any medium, provided the original work is properly cited.

1,4-Dihydropyridine (DHP), an important class of calcium antagonist, inhibits the influx of extracellular Ca^{+2} through L-type voltage-dependent calcium channels. Three-dimensional (3D) structure of calcium channel as a receptor for 1,4-dihydropyridine is a step in understanding its mode of action. Protein structure prediction and modeling tools are becoming integral parts of the standard toolkit in biological and biomedical research. So, homology modeling (HM) of calcium channel alpha-1C subunit as DHP receptor model was achieved. The 3D structure of potassium channel was used as template for HM process. The resulted dihydropyridine receptor model was checked by different means to assure stereochemical quality and structural integrity of the model. This model was achieved in an attempt to understand the mode of action of DHP calcium channel antagonist and in further computer-aided drug design (CADD) analysis. Also the structure-activity relationship (SAR) of DHPs as antihypertensive and antianginal agents was reviewed, summarized, and discussed.

1. Introduction

Voltage-gated calcium channels play an integral role in the entry of Ca^{2+} ions into excitable cells and are also involved in a variety of calcium-dependent processes, including muscle contraction, hormone or neurotransmitter release, gene expression, cell motility, cell division, and cell death [1, 2]. The isoform alpha-1C gives rise to long-lasting (L-type) calcium currents. They are blocked by 1,4-dihydropyridines (DHPs) such as nifedipine, phenylalkylamines such as verapamil, and benzothiazepines such as diltiazem [3]. Voltage-dependent calcium channels are multisubunit complexes, consisting of alpha-1, alpha-2, beta, and delta subunits in a 1:1:1:1 ratio. The channel activity is directed by the pore-forming and voltage-sensitive alpha-1 subunit. In many cases, this subunit is sufficient to generate voltage-sensitive calcium channel activity that displays the major electrophysiological and pharmacological properties of the full-fledged heteromeric channels [4–7].

DHP is the most feasible heterocyclic ring with various substitutions at several positions [8]. The discovery that the 1,4-dihydropyridine class of calcium channel blockers inhibits the Ca^{2+} influx represents a major therapeutic advance in the treatment of cardiovascular diseases, such as hypertension, angina pectoris, and other spastic smooth muscle diseases [9]. The most feasible position for substitution is the 4-position which exhibits various calcium channel antagonist activities [10] and the heterocyclic ring is the common feature for various pharmacological activities such as antihypertensive, antianginal [11, 12], antitumor [13], anti-inflammatory activity [14, 15], antitubercular activity [16], analgesic activity [17] and antithrombotic [18, 19]. It binds to L-type channel and also shows action by binding to N-type channel [20]. The DHP class of compounds, in which nifedipine is the prototype, has been the aim of many structure-activity relationship studies [21–28]. 1,4-DHP nucleus is capable of recognizing comparatively small

	1	10	20	30	40	50	60					
2A9H	A	LHWR	A	AGAA	TVLLVIVLL	LAGSYLAV	LAER	GAPGAA	-----	LISYPDAL	WWSVETAT	TV
model	I	KAMVP	LLHI	ALLVLFV	I I I Y A I I G I	ELFMG	KMHK	TCYNGITN	FDNF	AFAFAM	LTVFQCIT	ME
	70	80	90	100	110	120						
2A9H	GYGDL	YPVT	-----	LWGRCVA	VVVMVA	GITSYGLVFAAV	ATWVFG	REQ	ALHWR	AAGAA	T	
model	GWTDV	LYWV	NDAVGRD	WPVIYFV	TLII	GSFFVLNLV	LGVLS	GEFSKERE	LNSVRS	IAS	LL	
	130	140	150	160	170	180						
2A9H	VLLVI	VLLAG	SYLAV	LAER	-GAPGAA	-----	LISYPDAL	WWSVETAT	TTVGYGDL	YPVT	-	
model	LLLFL	FIIIFS	SLIGMQL	FGGKFN	FDEMQ	TRRST	FDNF	FQSL	LTVFQ	IL	TGEDWNS	VMYDGI
	190	200	210	220	230	240						
2A9H	-----	LWGRCVA	VVVMVA	GITSYGLVFAAV	ATWVFG	REQ	ALHWR	AAGAA	TVLLVIV			
model	MAYGGP	SFPGML	VLCIYFI	ILFICG	NYILLN	VFLAIAVDN	LADAEFVA	IR	TIGNI	VIVTLL		
	250	260	270	280	290	300						
2A9H	LLAGSYLAV	LAER	GAPGAA	-----	LISYPDAL	WWSVETAT	TTVGYGDL	YPVT	-----			
model	QFMFAC	IGVQLFK	GKLYTCS	SDSKFD	FDNVLA	AAMALFTV	STFEGWPEL	LYRS	ID	SHTEDK		
	310	320	330	340	350	360						
2A9H	-----	LWGRCVA	VVVMVA	AGITSYGLVFAAVA	TWVFGRE	QALHWR	AAGAA	TVLLVIVL	IA			
model	GPIYNYR	VEISIF	FI I Y I I I	I A F F M N	I F V G F V	I V T F Q E Q	G I K S F Q A	L P Y V A L L	I V M L F H I			
	370	380	390	400	410	420						
2A9H	GSYLAV	LAER	-GAPGAA	-----	LISYPDAL	WWSVETAT	TTVGYGDL	YPVT	-----			
model	YAVIGM	QVFGKIA	LN	DTTEINRNN	EQTFPQAV	LLLFRCAT	GEAWQD	IMLACMP	GKKCAPE			
	430	440	450	460	470	480						
2A9H	-----	LWGRCVA	VVVMVA	AGITSYGLVFAAV	ATWVFG	REQ						
model	S	E P S N S T E G E T P C G S S	F A V F Y F I S F Y M L C A F L I I N L F V A V	I M D N F D Y L T								

FIGURE 1: Sequence alignment between the amino acid sequence of model and that of KcsA. Red lines are chain break, dashes are inserted gaps, color code: blue = identical, sky blue = similar (color intensity decreases with similarity decrease), and white = no similarity; model = DHP receptor model amino acid sequence; 2A9H = the amino acid sequence of the template KcsA; numbers from 1 to 480 are amino acid sequence ruler.

differences in sequence associated with the generation of Ca^{2+} channels splice variants [29].

The number of known protein sequences is 50 times as that of the 3D protein structures. This gap hinders evolution in many areas of biochemistry because a protein sequence provides little meaning outside the context of its 3D structure. The disparity is less severe than the numbers might suggest because different proteins often adopt similar 3D folds [30]. As a result, each new protein structure can serve as a model for other protein structures. As an approach to understand the mechanism of action of DHPs, splicing veracity, and selectivity, 3D structure of L-type voltage-gated Ca^{2+} channel alpha-1C was developed by means of homology modeling. Furthermore, SAR of DHP was reviewed, summarized, and discussed.

2. Experimental Protocol

The protocol used to develop the DHP model is divided into three phases: sequence alignment, model construction, and model evaluation.

2.1. Sequence Alignment. The model was constructed using amino acid sequence of voltage-dependent L-type calcium channel subunit alpha-1C (code CACIC.HUMAN Q13936 isoform 20) obtained from UniProtKB/Swiss-Prot sequence database [31, 32]. Coordinates of potassium channel KcsA

atoms in their closed conformation were downloaded from the RCSB Protein Data Bank (code 2A9H) [33]. Amino acid sequences of S5, S6, and P-loops in between for the four repeats (I–IV) (262–413, 645–760, 1023–1173, and 1354–1483, resp.) were used for sequence alignment with the amino acid sequence of KcsA as proposed by Zhorov et al. [34] (c.f. Figure 1).

In order to favor valid superimposition of the residues, the sequence of each repeats was organized as S5, S6, and P-loop, allowing for a more flexible inspection of the results and easier corrections (c.f. Table 1). The amino acid sequence of repeats I and III, has long extracellular loop which would decrease the quality of the generated model, so amino acid sequences (301–341 and 1064–1095) were excluded from repeats I and III, respectively. Since the template is 88 residues shorter than the target protein, gaps were inserted to achieve best sequence similarity and identity without affecting sequence alignment proposed by Zhorov et al. [34].

2.2. Construction of the DHP Receptor Model. The modeling procedure consisted of two steps: model construction from template and refinement of loops. The above described sequence alignment file was used as input for the MODELLER 9v4 program [35] with the high-resolution NMR structure of potassium channel KcsA available in the RCSB Protein Data Bank (PDB entry 2A9H) as template for the 3D structure. Molecular modeling studies were performed

TABLE 1: Amino acid sequences of L-type voltage-gated Ca^{2+} channel α -1C and potassium channel (KcsA) used for homology modeling of DHP receptor.

S5					
KcsA	23	ALHWRAAGAA	TVLLVIVLLA	GSYLAVLAER	GAP GAA-
Repeat I	262	I KAMVP L LH I	ALLVLFVI I I	YAI I G LELFM	GKMHKT-
Repeat II	645	LNS VR S I A S L	LLLLF LFI I I	FSLGMLQFLG	GKFNFD E
Repeat III	1023	FVA I R T I G N I	VIV <u>T</u> T LLQFM	FACI GVQLF K	GKLYTC-
Repeat IV	1354	I KS FQ A LP YV	ALLIV MLFF I	YAVI GMQVFG	KIALNDT
P-loop					
KcsA	59	L I SYPDALWW	SVETATTVGY	GDLY P VT - - -	
Repeat I	298	CYN ³⁴² GI TNF D N	FAFAMLTVFQ	C I TMEGWTDV	L YWVNDAVG R
Repeat II	682	MQTRRSTF D N	FPQS L LTVFQ	I LT G EDWNSV	MYD G I MAYGG PSFPG - - - -
Repeat III	1059	SDSSK ¹⁰⁹⁶ DFD N	VLAAMMALFT	VS T F EGWP EL	L Y R S I D S HTE DKGPIYNYR
Repeat IV	1391	T E INRN NN FQ	TF PQA V LLLF	RC AT GEAWQD	I ML ACM PGKK CAPESEPSNS TEGETPCGS
S6					
KcsA	86	LWGRCVAVVV	MVAGITSYGL	V FAAVATWF V	GREQ
Repeat I	379	DWPWIY FV T L	I II GSFFV <u>L</u> N	LVLGV LS G E F	SKERE
Repeat II	727	MLVC IY F I I L	F I CGNYI <u>L</u> L N	VFLA I AV D N L	ADAE
Repeat III	1140	V E I S IF F I I <u>Y</u>	I III AFFM <u>M</u> N	IFVGFVIVTF	QEQG
Repeat IV	1450	SFAVFYFISF	YMLCAFLI <u>I</u> N	LFVAVIMDNF	DYLT

(i) Residue number is in the left of one letter code for the first residue and site of exclusion.

(ii) Active site residues are bold and underlined.

using the Accelrys Discovery Studio structure modeling package version 2.5 running on Intel Core 2 Duo CPU personal computer. The model sequence, template structure, and sequence alignment were used as input files to build the model. Loops can be defined automatically from the model to a template sequence alignment. The MODELER Loop Refinement-DOPE-Loop method [36] was used for initial refinement of the loop conformation after model generation. The model side-chain conformation was optimized based on systematic searching of side-chain conformation and CHARMM energy minimization using the ChiRotor algorithm [37]. Five models were obtained from the first step of molecular modeling. These models were subjected to a comparison based on the best scores to reveal the differences among them. The model with the lowest energy and the lowest restraint violation was selected for the second step.

Secondly, the loops between helices were subjected to refinement while keeping the start and end residues constrained. This procedure is based on the idea that transmembrane helices are much less flexible than loops, thus permitting to produce a sounder core alignment if the integrity of the helices is conserved. The more unpredictable loops can bear the more important differences. A CHARMM-based protocol [38] that optimizes the conformation of a contiguous segment (i.e., a loop) of a protein structure was used for loop refinement. It is based on systematic conformational sampling of the loop backbone and CHARMM energy minimization. This approach can be used to refine a loop structure from a homology model as well as to optimize a segment of the protein experimental structure where the structure is poorly defined.

The homology modeling (HM) phase was followed by the model evaluation phase. The stereochemical quality and structural integrity of the model were tested by RAMPAGE, ERRAT, MolProbity, ProSA, and Verify3D software.

2.3. Calcium Binding. Finally, the hydrogen atoms were added to the structure. The AMBER force field parameters were applied for the whole structure and the calcium ions were used. The four glutamate residues in the selectivity filter (Glu³⁶³, Glu⁷⁰⁶, Glu¹¹³⁵, and Glu¹⁴⁶⁴) were charged with CHARMM-based algorithm [39]. The system was neutralized by adding an appropriate number of counter ions. The model was completed with the addition of the two calcium cations coordinated with the charged glutamate residues in selectivity filter.

3. Results and Discussion

3.1. Sequence Alignment. Beside the choice of the reference, the accuracy of the alignment is the most crucial step in assuring the quality of the homology modeling. An accurate sequence alignment between the model and the template proteins is essential to achieve high quality models. Voltage-gated Ca^{2+} channels are members of a gene superfamily of transmembrane ion channel proteins that includes voltage-gated K^+ and Na^+ channels. Ca^{2+} channels share structural similarities with K^+ and Na^+ channels in that they possess a pore-forming α_1 subunit in four repeats of a domain with six transmembrane-spanning segments that include the voltage-sensing S4 segment and the pore-forming (P) region. As

no atomic resolution images of calcium channel structures exist, much has been learnt about their structure since the recent determination of crystal structures of a number of potassium channels [40, 41]. The α_1 subunit contains four repeated domains (I–IV), each of which includes six transmembrane segments (S1–S6) and a membrane associated loop (the “P-loop”) between segments S5 and S6. The four repeated domains are also remarkably similar to those known to form the voltage-gated potassium channels. However, potassium α_1 subunit is homotetramer and calcium channel is heterotetramer. Potassium channel KcsA (PDB code 2A9H) has been selected to be the template. Amino acid sequences of S5, S6, and P-loops in between for the four repeats (I–IV) (262–413, 645–760, 1023–1173, and 1354–1483, resp.) of voltage-dependent L-type calcium channel subunit alpha-1C (code CACIC.HUMAN Q13936 isoform 20) were used for sequence alignment with the amino acid sequence of KcsA as proposed by Zhorov et al. [34], where S6 segments of LCC are aligned with M2 segments of KcsA in a manner similar to the alignment of the Na⁺ channel with KcsA described by Lipkind and Fozzard [42] and S5s were aligned with the M1 segment of KcsA as proposed by Huber et al. [43] and the P-loops were aligned using MULTALIN server [44]. Proteins that fold into similar structures can have large differences in the size and shape of residues at equivalent positions. These changes are tolerated not only because of replacements or movements in nearby side chains, as explored by Ponder and Richards, but also as a result of shifts in the backbone [30]. For a more flexible inspection, the sequence of each repeat was organized as S5, S6, and P-loop, allowing easier corrections (c.f. Table 1). The amino acid sequence of repeats I and III has long extracellular loop which would reduce the quality of the generated model, so amino acid sequences (300–342 and 1083–1116) were excluded from repeats I and III, respectively. Since the template is 88 residues shorter than the target protein, gaps were inserted to achieve best sequence similarity and identity without affecting sequence alignment proposed by Zhorov et al. [34]. The greatest attention was thus paid to the careful construction of transmembrane helices S5 and S6 and P-loop as well.

3.2. Construction of the DHP Receptor Model. Although the two proteins have low sequence identity of 9.5% and sequence similarity of 29.2%, the MODELLER program was applied to generate satisfactory models. As an integral process of model building, initial refinement of the loop conformation after model generation was automatically performed by MODELLER Loop Refinement-DOPE-Loop method during the process. The model achieved from the alignments by Zhorov et al. [34] was subjected to extensive loop optimization. This procedure is based on the idea that transmembrane helices are much less flexible than loops, thus permitting to produce a sounder core alignment if the integrity of the helices is conserved. On the contrary, the more volatile loops can bear the more important difference between the coordinates of the reference and the model. When a homology model is created, there are parts of the model sequence which are not aligned to any template structures. For these sections, no

homology restraints (such as C α -C α distance restraints) can be applied. These parts of the structure generally have greater errors compared to the regions which are modeled based on a template structure. In attempts to reduce these errors, a CHARMM-based protocol that optimizes the conformation of a contiguous segment (i.e., a loop) of a protein structure called loop refinement was applied [38]. This is based on systematic conformational sampling of the loop backbone and CHARMM energy minimization. The algorithm goes through three stages: construction and optimization of loop backbone, construction of loop side-chain, and optimization of loop followed by reranking of the conformations. The model was then checked after a thorough energy minimization designed to reduce the steric clashes of the side chains without modifying the backbone of the protein to solve these contacts. To avoid modification of the backbone of the protein, the optimization of the geometry of side chain was performed with constraining the backbone. After the optimization, models were checked to assess the quality of their structure.

3.3. Model Evaluation. To assess stereochemical quality and structural integrity of the model, RAMPAGE [45], ERRAT [46], MolProbity [47–49], ProSA [50, 51], and Verify3D [30, 52] software were used. For comparison, these methods were also used to evaluate the template structure, and then each repeat was examined separately by means of ProSA. RAMPAGE is an offshoot of RAPPER which generates a Ramachandran plot using data derived by Lovell et al. [45]. It is recommended that it be used for this purpose in preference to PROCHECK, which is based on much older data. The Ramachandran diagram plots phi versus psi dihedral angles for each residue in the protein. The diagram is divided into favored, allowed, and disallowed regions, whose contouring is based on density-dependent smoothing for 81234 non-Glycine, non-Proline residues with B < 30 from 500 high-resolution protein structures. Regions are also defined for Glycine, Proline, and pre-Proline as shown in Figures 2 and 3.

ERRAT is a protein structure verification algorithm, that is, especially well-suited for differentiating between correctly and incorrectly determined regions of protein structures based on characteristic atomic interactions [46]. Different types of atoms (C, N, and O) are distributed nonrandomly with respect to each other in proteins because of energetic and geometric effects. Errors in model building lead to more randomized distributions of the different atom types, which can be distinguished from correct distributions by statistical methods. The program works by analyzing the statistics of nonbonded interactions between different atom types. A single output plot is produced that gives the value of the error function versus position of a 9-residue sliding window. In comparison with statistics from highly refined structures, the error values have been calibrated to give confidence limits. The program provides an “overall quality factor” value which is defined as the percentage of the protein for which the calculated error value falls below the 95% statistical rejection limit (c.f. Table 2). The ERRAT overall quality factors of

TABLE 2: Assessment scores for the DHP receptor model compared to the template.

Items	Model	Template	Comment
ERRAT	77.37	86.24	ERRAT overall quality factor
ProSA	-3.66	-3.63	ProSA Z-score as average of the four repeats
Verify3D	66.46% (W)	69.39% (W)	Percentage of residues with Verify3D average score > 0.2; Verify3D overall assessment of the structure (P = pass, W = warning, or F = fail) shown in parentheses

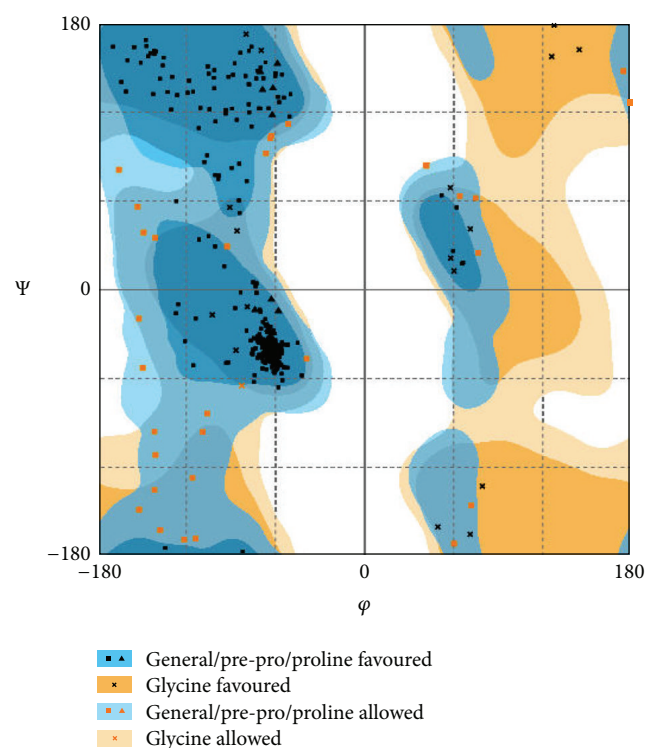


FIGURE 2: Ramachandran plot. The plot of DHP receptor model shows that 92.9% of residues were found in the favored, 7.1% in the allowed, and none in the outlier regions.

the model and template are given. The ERRAT score of the model was lower than that of template. This is not surprising since the model has longer loops than template. This method provides a useful tool for model building, structure verification, and making decisions about reliability. A more reliable discrimination of incorrect regions would likely be obtained by combining the present analysis with others.

ProSA and Verify3D are two methods that are sensitive in distinguishing between overall correct fold and those with an incorrect fold [53]. ProSA-Protein Structure Analysis program is a diagnostic tool that is based on the statistical analysis of all available protein structures [50, 51]. It is a tool widely used to check 3D models of protein structures for potential errors. Its range of application includes error recognition in experimentally determined structures [54, 55], theoretical models [56, 57], and protein engineering [58, 59]. The energy of the structure is evaluated using a

distance-based pair potential and a potential that captures the solvent exposure of protein residues. From these energies, two characteristics are derived and displayed: Z-score and a plot of residue energies. The Z-score indicates overall model quality and measures the deviation of the total energy of the structure with respect to an energy distribution derived from random conformations. Z-scores outside a range characteristic of native proteins indicate erroneous structures. The overall quality score calculated by ProSA for a specific structure is displayed in a plot that shows the scores computed from all experimentally determined protein chains currently available in the Protein Data Bank (PDB). Structures which contain errors are likely to have Z-score outside the range of values characteristic of native proteins [50, 51]. Table 2 lists the Z-score calculated by ProSA (as average of the four repeats Z-score) for the model and compared against the template. The Z-scores for the model and template are much closer to the middle region of scores observed for experimentally determined protein structures in the PDB including the template structure. The energy plot shows the local model quality by plotting energies as a function of amino acid sequence. In general, positive values correspond to problematic or erroneous parts of the model (c.f. Figure 4).

Verify3D analyzes the compatibility of an atomic model (3D) with its own amino acid sequence (1D) and hence tests the accuracy of the model. Each residue is assigned a structural class based on its location and environment. The environments are described by the area of the residue buried in the protein and inaccessible to solvent, the fraction of side-chain area that is covered by polar atoms (O and N), and the local secondary structure. Based on these parameters, each residue position is categorized into an environmental class. In this manner, a 3D protein structure is converted into a 1D string, like a sequence, which represents the environmental class of each residue in the folded protein structure. A collection of good structures is used as a reference to obtain a score for each of the 20 amino acids in this structural class. The scores of a sliding 21-residue window are added and plotted for individual residues. This method evaluates the fitness of a protein sequence in its current 3D environment. It can be applied to assess the quality of a theoretical model or to examine the characteristics of an experimental structure [30, 52]. The model was evaluated and compared with the template. The model and the template had the same rating and the percentage of the model was comparable to that of the template. Table 2 shows the percentage of residues that had an average score > 0.2 and the Verify3D assessment of the structure (pass, warning, or fail) for the model and

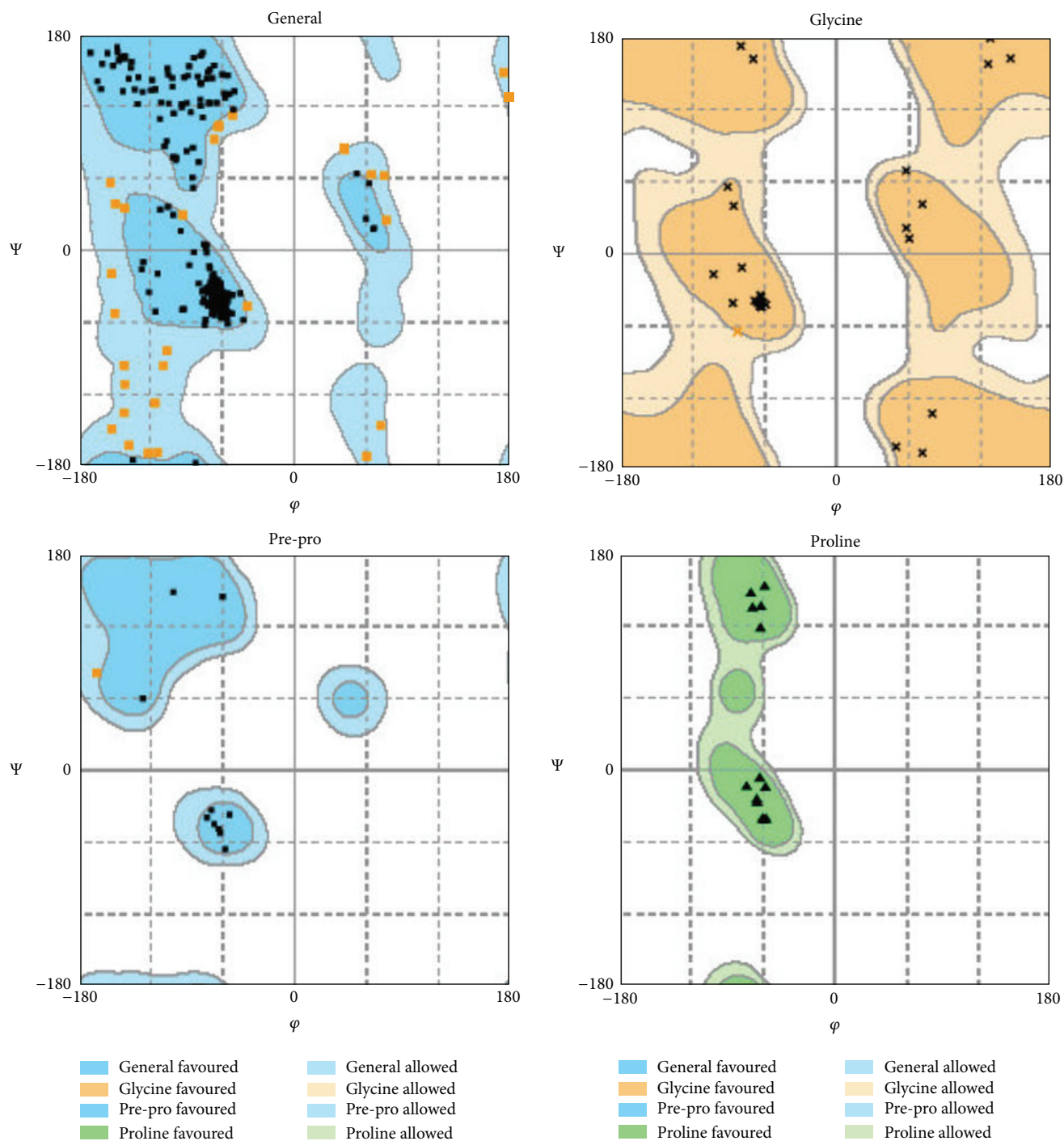


FIGURE 3: Ramachandran plot. The plot shows general, glycine, pre-proline, and proline for DHP receptor model and no outlier was seen.

template. Figure 5 shows the Verify3D profile for the model structure. Residues with a score over 0.2 should be considered reliable and the sequences exhibiting lower scores are those of extracellular loops.

MolProbity is a program for quality validation of 3D structures of proteins, nucleic acids, and complexes [47–49]. It provides detailed all-atom contact analysis of any steric

problems within the molecules and can calculate and display the H-bond and van der Waals contacts in the interfaces between components. Using the method of Lovell et al. [45], torsion angles are plotted on four Ramachandran plots—“general” for all non-Pro and non-Gly residues, “Gly”, “Pro”, and “pre-Pro” for residues preceding Pro. MolProbity also determines $C\beta$ deviations and the distance from the modeled

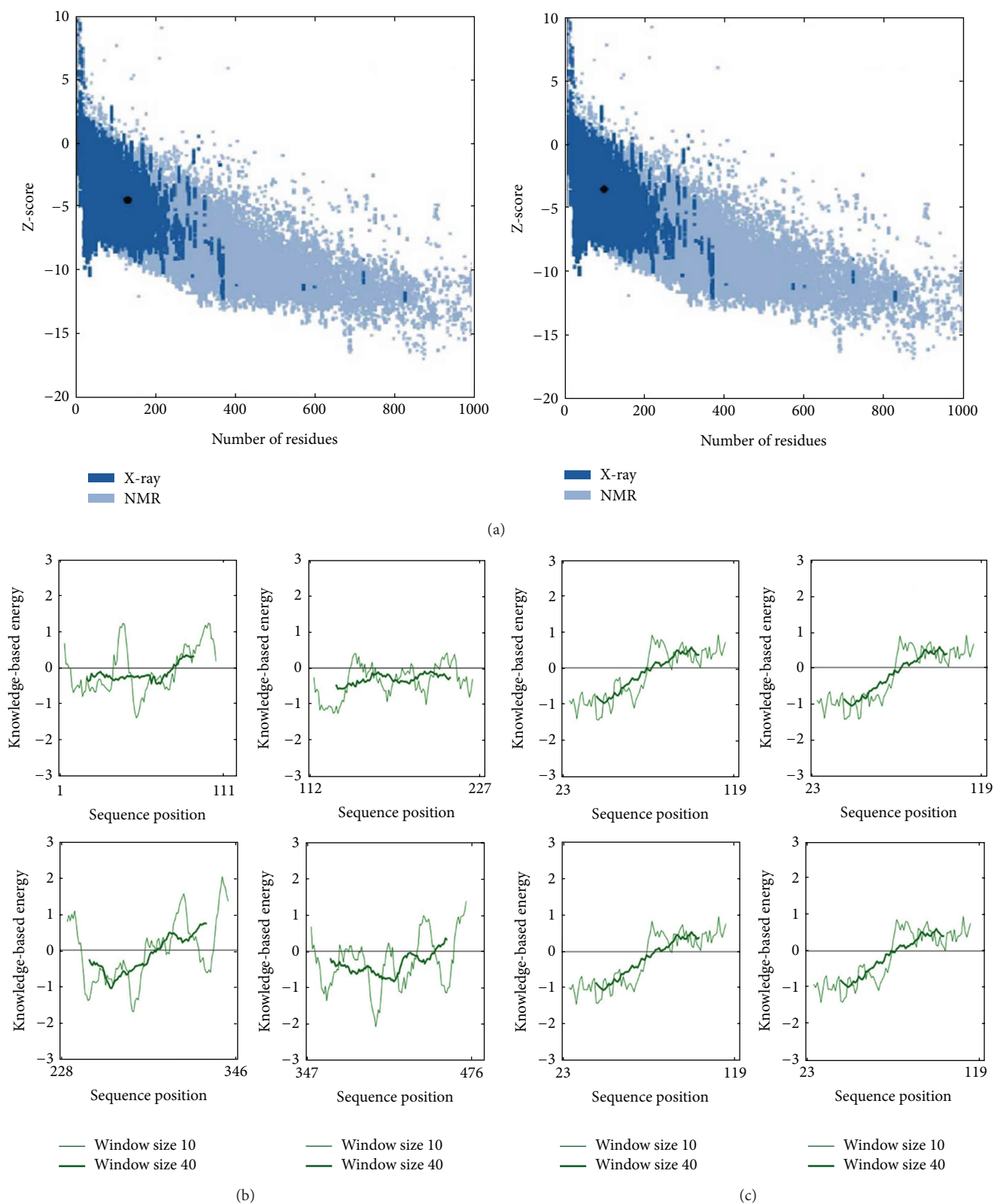


FIGURE 4: ProSA plot. Each repeat was examined separately. (a) ProSA Z-scores for DHP receptor model (left) template (right) and the complete PDB as a function of protein length. Blue and sky blue dots are Z-scores of PDB structures determined by X-ray crystallography and NMR, respectively; (b) ProSA energy profiles for DHP receptor model (four repeats) and (c) ProSA energy profiles for template (four repeats). Negative scores indicate a high quality model.

TABLE 3: MolProbity assessment of DHP receptor model compared to the template.

Items	Model	Template	Comment
Favored	91.67	81.32	Percentage of residues with phi-psi angle combinations that lie in the favored regions of the Ramachandran plots
Allowed	7.9	17.1	Percentage of residues with phi-psi angle combinations that lie in the allowed regions of the Ramachandran plots (outside the favored regions but not in the disallowed regions)
Outliers	0.43	1.58	Percentage of residues with phi-psi angle combinations that lie in the disallowed regions of the Ramachandran plots; the actual number of outlier residues is shown in parentheses
$C\beta$	30.27	0	Number of residues with $C\beta$ deviations $\geq 0.25\text{\AA}$
Bond length	0	0	Percentage of backbone bond lengths > 4 standard deviations from the accepted values
Bond angle	0.25	0	Percentage of backbone bond angles > 4 standard deviations from the accepted values
Clash-score	40.52	4.14	Number of atomic clashes per 1000 atoms
Percentile	8	96	Percentile rank compared to structures in the PDB within a similar resolution range

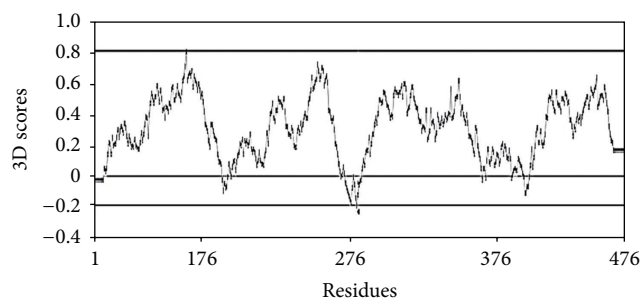


FIGURE 5: Verify3D score profile calculated for DHP receptor model. Scores over 0.2 indicate a high quality model.

$C\beta$ position to the ideal position calculated from backbone coordinates. $C\beta$ deviation is actually a measure of geometric nonideality around $C\alpha$ that often indicates incompatibility between side chain and main chain conformations [45, 48]. $C\beta$ deviations of $\geq 0.25\text{\AA}$ are often correlated with some form of local misfitting in the model [47].

Finally, MolProbity provides a clash score as a result of an all-atom contact analysis which is performed after adding hydrogen atoms, both polar and nonpolar, to a structure [47]. When non-donor-acceptor atoms overlap by more than 0.4\AA , at least one of the two atoms must be modeled incorrectly. A clash at this location is noted and incorporated into the clash score, which is simply the number of clashes per 1000 atoms. A structure's clash score percentile rank, compared to structures in the PDB within a similar resolution range, is also calculated. Percentile score for the template and the model was calculated as shown in Table 3.

Neither the template nor the model had $>98\%$ of residues in the favored regions, but the percentages for the model were better compared to those of the templates. The model had outlier 0.43% compared to the template that has 1.58% . All bond lengths were deemed acceptable by MolProbity, being within 4 standard deviations of the values determined

by Engh and Huber [60]. It is expected that a modeled or experimentally determined structure should have $<0.1\%$ of bond angles that differ from the accepted values, but the model had percentage above this value. The elevated percentage is due to residues in the extracellular loops away from the core of the model structure. MolProbity provides a count of residues for which the $C\beta$ position deviates by $\geq 0.25\text{\AA}$ from the ideal position; ideally there should be no such residues in a structure. This is the case only for the template. There are $30.27\ C\beta$ deviations in the model, likely indicating geometric problems around the alpha carbons, but again they are away from the core of the model structure, in the terminal residues of each chain and in the extracellular loops. The models had rather high clash scores, putting the structures of no higher than the 8 percentile for PDB structures at all resolutions. This clearly points to structural problems in the homology model since atomic clashes cannot occur in actual molecules. It is not surprising that the quality of the homology model would be lowest in the regions where model sequence has a lower degree of identity with the template.

Taken together, all of the above data indicate that the quality of the model is similar to that of the template. The model can be used for further computer-aided drug design (CADD) and it can be used in understanding how DHP work at the molecular level.

3.4. Selectivity Filter "Calcium Cofactor". The pore-forming alpha-1 subunit of L-type voltage-gated Ca^{2+} channel contains Ca^{2+} binding site that is allosterically coupled to the receptor site for DHP calcium antagonists. Permeation of Ca^{2+} through the pore of the calcium channel is thought to require the binding of two calcium ions. The first ion binds and blocks the pore while the second binds and allows permeation [61]. Glutamate residues in the pore of the Ca^{2+} channel are required to bind one Ca^{2+} ion for generating the high affinity state for DHP antagonists. Four glutamate

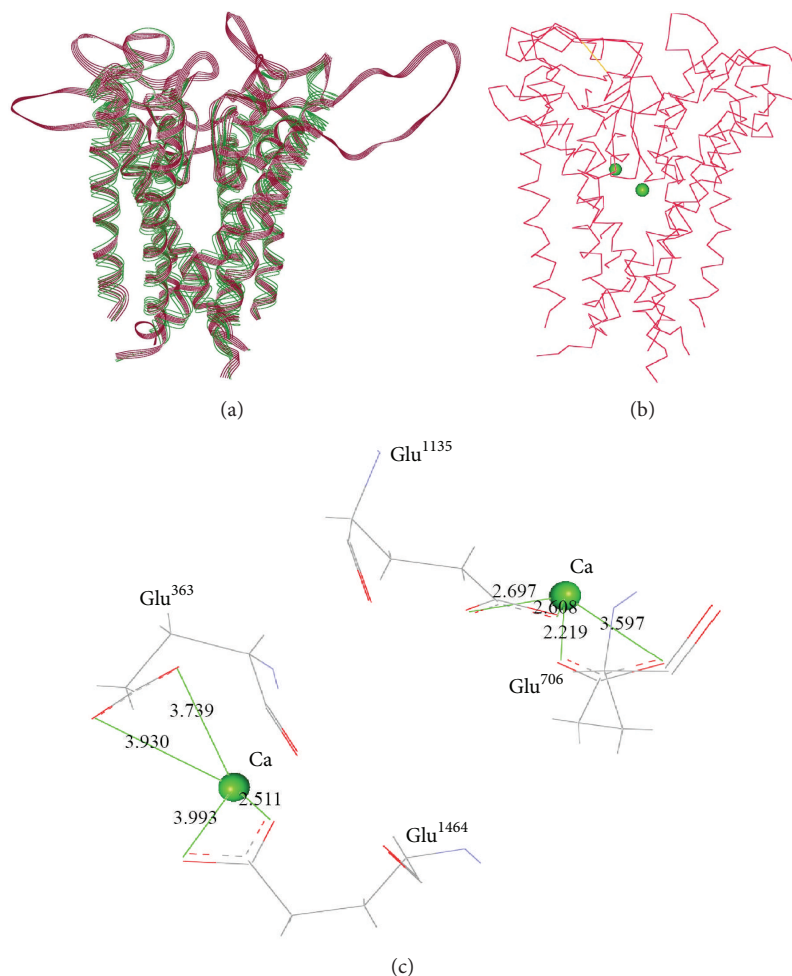


FIGURE 6: 3D structure of DHP receptor model. (a) Superimposition between template (green) and the model of DHP receptor (red), line ribbon presentation; (b) C alpha stick presentation of 3D structure of DHP receptor model showing the two calcium ions position; (c) selectivity filter glutamate residues make salt bridge with calcium ions (green CPK style).

residues are involved in the selectivity filter. Two calcium ions are incorporated. One calcium ion makes salt bridge between Glu³⁶³ and Glu¹⁴⁶⁴. The other one makes salt bridge between Glu⁷⁰⁶ and Glu¹¹³⁵. The distance between the carboxylic group and calcium ion ranges from 2.219 Å to 3.993 Å, as shown in Figure 6.

3.5. Structure Activity Relationship Assessment. The presence of 1,4-DHP ring, as an essential moiety for calcium antagonist activity, has been assured in many literatures [20, 62]. Some investigations revealed that dihydropyrimidine ring could be used in place of 1,4-DHP ring [63]. Both 1,4-DHP and dihydropyrimidine rings adopt boat conformation with hydrogen atom attached to Sp³-hybridized nitrogen. Ring oxidation or N¹ substitution abolishes activity. Oxidation of the ring, protonation of N¹, or substitution at this position changes boat conformation and the position of hydrogen bonding. So, this hydrogen atom is involved in a direct interaction with the receptor. N–H at position-1 is a hydrogen bond donor. Hydrogen bond acceptors in the receptor involve Thr¹⁰³⁶, Tyr¹¹⁴⁹,

and Tyr¹⁴⁶⁰. The first two residues (Thr¹⁰³⁶ and Tyr¹¹⁴⁹) were found to be essential for DHP binding since mutations T¹⁰³⁶Y and Y¹¹⁴⁹A result in no binding with DHP. Interestingly, mutation of threonine to tyrosine only replaces aliphatic hydroxyl group with aromatic one which postulates that not only is the hydroxyl group required for interaction but also its position is crucial. Tyrosine phenyl group is bulky and would disrupt the DHP interaction site [64]. Tyr¹¹⁴⁹ makes H-bond with the N–H group of DHP ring [34, 65], while Thr¹⁰³⁶ was found to be important for the integrity of interaction site and not involved in a direct interaction with DHPs [64].

Substitution at 2,6-positions of 1,4-DHP ring should be lower alkyl group [20, 62]; however, recent studies revealed that one bulky group like phenyl group at C-6 position increased activity and selectivity due to its interaction with

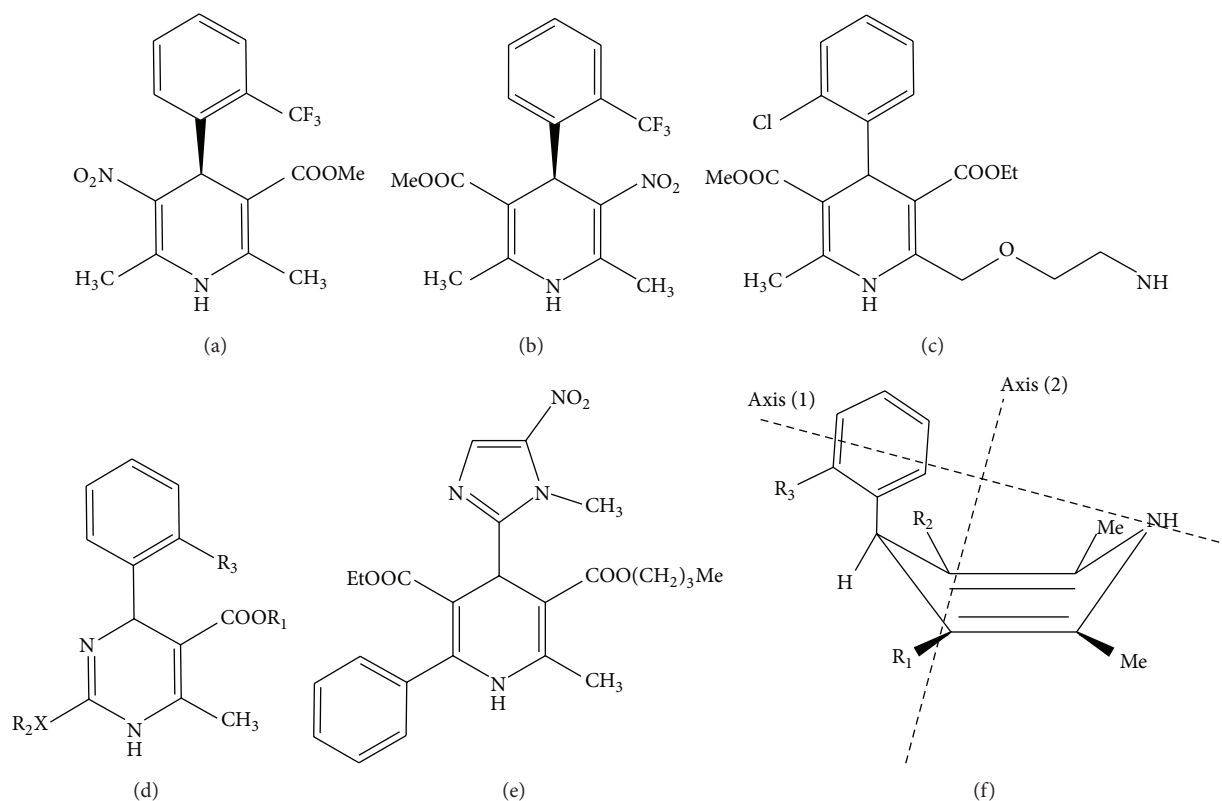


FIGURE 7: Structures of some DHP receptor modulators: (a) (S)-Bay K8644 (agonist); (b) (R)-Bay K8644 (antagonist); (c) amlodipine; (d) dihydropyrimidine (general structure); (e) highly active compound with phenyl substituent at C-6 position; and (f) 1,4-DHPs general structure showing the orientation of affinity axis (axis 1) and chirality-activity axis (axis 2) on the boat conformation.

high lipophilic pocket in the receptor. These lipophilic aromatic substituents attached to the C-6 position of 1,4-DHP ring are supposed to improve penetration into organs; these compounds are more active as compared with similar compounds that contain methyl moiety in C-6 position (c.f. Figure 7). On the other hand, the activity data indicate a decrease in activity when the methyl group at C-2 position is replaced by a phenyl substituent [66]. This observation of decreasing activity is in contrast to the effect of increasing lipophilicity. This is due to the increase in steric hindrance by phenyl group. So, there is a challenge to make a suitable balance between lipophilicity and steric hindrance for the calcium channel antagonist activity of DHPs [22]. The C-2 methyl substituent makes lipophilic interaction with Ile¹⁰⁵⁰, while C-6 position can tolerate bulkier groups. The phenyl group can be accommodated by a highly lipophilic pocket in the receptor. One amino group is tolerated and can increase activity due to hydrogen bonding with the receptor and plasma protein which leads to slow dissociation from the receptor and from blood, respectively. The amino group at C-2, such as amlodipine, imparts aqueous solubility and ionization at physiological pH [67].

Ester groups at C-3 and C-5 positions show optimum activity. Ester group is involved in coordination with glutamate residues through calcium ion bridge, a part of

selectivity filter. Absence of calcium ion greatly decreases DHP binding to the receptor [61]. Replacement of C-3 ester with ketone or nitrile group greatly reduces activity due to replacement of bidentate chelating ester group with monodentate chelating ketone group and nonchelating nitrile group. The presence of electron-withdrawing groups shows decreased antagonistic activity and may even show agonist activity. R and S Bay K8644 are evidence on dual 1,4-DHP functional activity, agonist and antagonist. The lipophilic gate bracelet (Met¹¹⁵⁸, Leu³⁹⁷, Leu⁷⁴⁵, and Ile¹⁴⁶⁸) acts as a barrier that regulates the channel activity. Lipophilic gate bracelet and hydrophilic selectivity filter integrate the receptor ability to recognize difference between enantiomers. This would form enantiomeric selectivity axis (c.f. Figure 7). Enantiomeric selectivity of the channel is due to different nature of its active site between lipophilic gate bracelet and hydrophilic selectivity filter. On Bay K8644, C-3 ester lipophilic substitution results in antagonist activity while hydrophilic groups like nitrile or nitro group result in agonist activity.

C-4 substitution with heteroaromatic ring shows higher activity than compounds with alkyl or cycloalkyl substituents. Heteroaromatic rings are engaged in ring-to-ring interaction with Tyr⁴³¹¹. The first aromatic ring used was *ortho*-nitrophenyl as shown by the prototype nifedipine. Other heteroaromatic rings were used such as imidazole [68–72],

2,1,3-benzoxadiazole [73], 2,3-methylenebisoxypyrene [74], 5-phenylisoxazole [75], chloroindole [76], chlorobenzene [77], and 2,3-dichlorobenzene [78].

Compounds with *ortho*- or *meta*-substitution of electron-withdrawing nature possess optimum activity, while *para*-substitution shows decrease in activity according to its electronic and steric effect. The importance of the *ortho*- and *meta*-substituents is to “lock” the conformation of the 1,4-DHP such that the C-4 position aromatic ring is perpendicular to the 1,4-DHP ring. This perpendicular conformation has been proposed to be essential for the activity of the 1,4-DHPs [79].

From the above discussions, the 1,4-DHPs structure has two axes: affinity axis and chirality-activity axis (c.f. Figure 8). Affinity axis is in charge of binding to the receptor and consists of N-H group and C-4 position aromatic substitution. Chirality-activity axis is composed of the two ester functional groups of substituents at C-3 and C-5 positions of the DHP ring. It is responsible for distinguishing the activity, agonist and antagonist, and also enantiomeric selectivity; that is, some enantiomers are more active than the others. The two axes are cross not parallel (c.f. Figures 7 and 8).

4. Conclusions and Future Directions

Voltage-gated Ca^{2+} channels play an integral role in the entry of calcium ions into excitable cells which are involved in many physiological and pathological calcium-dependent processes. 3D structure model of L-type calcium channel α -1 subunit with similar quality to the template has been developed and validated. It can be used in further computer-aided drug design (CADD) for predicting and rationalizing 1,4-DHPs activity. 1,4-DHPs calcium channel modulators are used as antihypertensive and antianginal agents. Their structure-activity relationship was reviewed and discussed in detail in an attempt to clear how they modulate calcium channel activity. As future tasks, the available DHPs structures will be used to map the active site in approach to further understand the mechanism of action at the molecular level.

Conflict of Interests

The authors declare that there is no conflict of interests regarding the publication of the paper.

References

- [1] R. J. Miller, “Multiple calcium channels and neuronal function,” *Science*, vol. 235, no. 4784, pp. 46–52, 1987.
- [2] G. J. Augustine, M. P. Charlton, and S. J. Smith, “Calcium action in synaptic transmitter release,” *Annual Review of Neuroscience*, vol. 10, pp. 633–693, 1987.
- [3] V. Leuranguer, M. E. Mangoni, J. Nargeot, and S. Richard, “Inhibition of T-type and L-type calcium channels by mibefradil: physiologic and pharmacologic bases of cardiovascular effects,” *Journal of Cardiovascular Pharmacology*, vol. 37, no. 6, pp. 649–661, 2001.
- [4] D. Schultz, G. Mikala, A. Yatani et al., “Cloning, chromosomal localization, and functional expression of the α 1 subunit of the L-type voltage-dependent calcium channel from normal human heart,” *Proceedings of the National Academy of Sciences of the United States of America*, vol. 90, no. 13, pp. 6228–6232, 1993.
- [5] R. D. Zühlke, A. Bouron, N. M. Soldatov, and H. Reuter, “ Ca^{2+} channel sensitivity towards the blocker isradipine is affected by alternative splicing of the human α (1C) subunit gene,” *FEBS Letters*, vol. 427, no. 2, pp. 220–224, 1998.
- [6] N. M. Soldatov, A. Bouron, and H. Reuter, “Different voltage-dependent inhibition by dihydropyridines of human Ca^{2+} channel splice variants,” *Journal of Biological Chemistry*, vol. 270, no. 18, pp. 10540–10543, 1995.
- [7] N. M. Soldatov, R. D. Zühlke, A. Bouron, and H. Reuter, “Molecular structures involved in L-type calcium channel inactivation. Role of the carboxyl-terminal region encoded by exons 40–42 in α (1C) subunit in the kinetics and Ca^{2+} dependence of inactivation,” *Journal of Biological Chemistry*, vol. 272, no. 6, pp. 3560–3566, 1997.
- [8] G. Swarnalatha, G. Prasanthi, N. Sirisha, and C. Madhusudhana Chetty, “1,4-Dihydropyridines: a multifunctional molecule: a review,” *International Journal of ChemTech Research*, vol. 3, no. 1, pp. 75–89, 2011.
- [9] A. Fleckenstein, “Specific pharmacology of calcium in myocardium, cardiac pacemakers, and vascular smooth muscle,” *Annual Review of Pharmacology and Toxicology*, vol. 17, pp. 149–166, 1977.
- [10] D. J. Triggle, “Calcium channel antagonists: clinical uses—Past, present and future,” *Biochemical Pharmacology*, vol. 74, no. 1, pp. 1–9, 2007.
- [11] B. Loev, M. M. Goodman, K. M. Snader, R. Tedeschi, and E. Macko, “‘Hantzsch-type’ dihydropyridine hypotensive agents,” *Journal of Medicinal Chemistry*, vol. 17, no. 9, pp. 956–965, 1974.
- [12] J. G. Breitenbucher and G. Figliozzi, “Solid-phase synthesis of 4-aryl-1,4-dihydropyridines via the Hantzsch three component condensation,” *Tetrahedron Letters*, vol. 41, no. 22, pp. 4311–4315, 2000.
- [13] R. Boer and V. Gekeler, “Chemosensitizers in tumor therapy: new compounds promise better efficacy,” *Drugs of the Future*, vol. 20, no. 5, pp. 499–509, 1995.
- [14] V. M. Bryukhanov, F. Zverev Ya., and V. I. Elkin, “Effects of calcium antagonists on the development of inflammatory edema in rats,” *Experimental and Clinical Pharmacology*, vol. 57, no. 2, pp. 47–49, 1994.
- [15] S. Bahekar and D. Shinde, “Synthesis and anti-inflammatory activity of 1,4-dihydropyridines,” *Acta Pharmaceutica*, vol. 52, no. 4, pp. 281–287, 2002.
- [16] G. A. Wächter, M. C. Davis, A. R. Martin, and S. G. Franzblau, “Antimycobacterial activity of substituted isosteres of pyridine- and pyrazinecarboxylic acids,” *Journal of Medicinal Chemistry*, vol. 41, no. 13, pp. 2436–2438, 1998.
- [17] S. Gullapalli and P. Ramarao, “L-type Ca^{2+} channel modulation by dihydropyridines potentiates κ -opioid receptor agonist induced acute analgesia and inhibits development of tolerance in rats,” *Neuropharmacology*, vol. 42, no. 4, pp. 467–475, 2002.
- [18] C. E. Sunkel, M. Fau de Casa-Juana, L. Santos et al., “4-Alkyl-1,4-dihydropyridines derivatives as specific PAF-acether antagonists,” *Journal of Medicinal Chemistry*, vol. 33, no. 12, pp. 3205–3210, 1990.

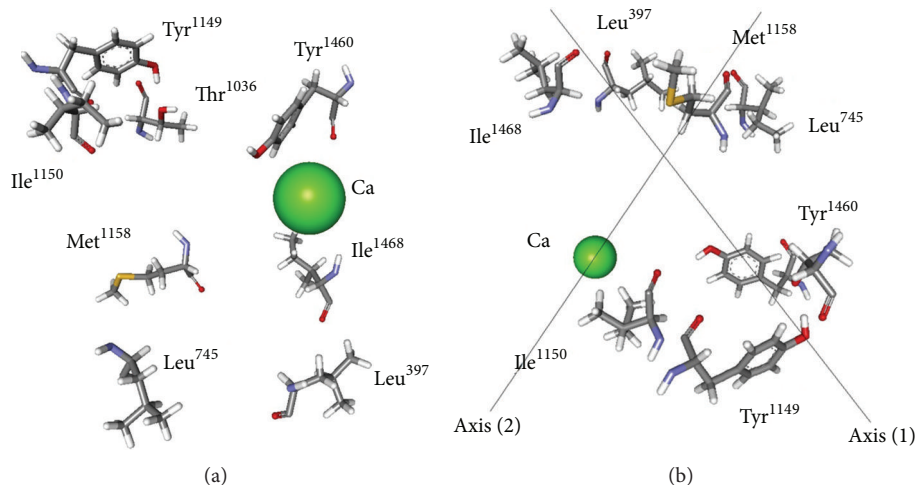


FIGURE 8: DHP receptor active site. (a) DHP sensing residues and calcium ion; (b) affinity axis passes through Tyr¹¹⁴⁹ (H-bond site) and Tyr¹⁴⁶⁰ (ring to ring interaction site); chirality-activity axis (axis 2) passes through water lake and calcium and hydrophobic bracelet (Leu³⁹⁷, Leu⁷⁴⁵, Met¹¹⁸⁵, and Ile¹⁴⁶⁸).

- [19] K. Cooper, M. J. Fray, M. J. Parry, K. Richardson, and J. Steele, "1,4-Dihydropyridines as antagonists of platelet activating factor. 1. Synthesis and structure-activity relationships of 2-(4-heterocycl)phenyl derivatives," *Journal of Medicinal Chemistry*, vol. 35, no. 17, pp. 3115–3129, 1992.
- [20] D. J. Triggle, "The pharmacology of ion channels: with particular reference to voltage-gated Ca²⁺ channels," *European Journal of Pharmacology*, vol. 375, no. 1–3, pp. 311–325, 1999.
- [21] B. Hemmateenejad, R. Miri, M. Akhond, and M. Shamsipur, "QSAR study of the calcium channel antagonist activity of some recently synthesized dihydropyridine derivatives. An application of genetic algorithm for variable selection in MLR and PLS methods," *Chemometrics and Intelligent Laboratory Systems*, vol. 64, no. 1, pp. 91–99, 2002.
- [22] B. Hemmateenejad, R. Miri, M. Akhond, and M. Shamsipur, "Quantitative structure-activity relationship study of recently synthesized 1,4-dihydropyridine calcium channel antagonists. Application of the Hansch analysis method," *Archiv der Pharmazie*, vol. 335, no. 10, pp. 472–480, 2002.
- [23] B. Hemmateenejad, M. Akhond, R. Miri, and M. Shamsipur, "Genetic algorithm applied to the selection of factors in principal component-artificial neural networks: application to QSAR study of calcium channel antagonist activity of 1,4-dihydropyridines (nifedipine analogues)," *Journal of Chemical Information and Computer Sciences*, vol. 43, no. 4, pp. 1328–1334, 2003.
- [24] B. Hemmateenejad, M. A. Safarpour, R. Miri, and F. Taghavi, "Application of ab initio theory to QSAR study of 1,4-dihydropyridine-based calcium channel blockers using GA-MLR and PC-GA-ANN procedures," *Journal of Computational Chemistry*, vol. 25, no. 12, pp. 1495–1503, 2004.
- [25] B. Hemmateenejad, R. Miri, M. A. Safarpour, M. Khoshneviszadeh, and N. Edraki, "Conformational analysis of some new derivatives of 4-nitroimidazolyl-1,4-dihydropyridine-based calcium channel blockers," *Journal of Molecular Structure*, vol. 717, no. 1–3, pp. 139–152, 2005.
- [26] R. Miri, K. Javidnia, A. Kebraie-Zadeh et al., "Synthesis and evaluation of pharmacological activities of 3,5-dialkyl 1,4-dihydro-2,6-dimethyl-4-nitroimidazole-3,5-pyridine dicarboxylates," *Archiv der Pharmazie*, vol. 336, no. 9, pp. 422–428, 2003.
- [27] L. Navidpour, H. Shafaroodi, R. Miri, A. R. Dehpour, and A. Shafiee, "Lipophilic 4-imidazolyl-1,4-dihydropyridines: synthesis, calcium channel antagonist activity and protection against pentylentetrazole-induced seizure," *Farmaco*, vol. 59, no. 4, pp. 261–269, 2004.
- [28] M. A. Safarpour, B. Hemmateenejad, R. Miri, and M. Jamali, "Quantum chemical-QSAR study of some newly synthesized 1,4-dihydropyridine calcium channel blockers," *QSAR and Combinatorial Science*, vol. 22, no. 9-10, pp. 997–1005, 2004.
- [29] D. J. Triggle, "1,4-Dihydropyridines as calcium channel ligands and privileged structures," *Cellular and Molecular Neurobiology*, vol. 23, no. 3, pp. 293–303, 2003.
- [30] J. U. Bowie, R. Lüthy, and D. Eisenberg, "A method to identify protein sequences that fold into a known three-dimensional structure," *Science*, vol. 253, no. 5016, pp. 164–170, 1991.
- [31] E. Perez-Reyes, X. Wei, A. Castellano, and L. Birnbaumer, "Molecular diversity of L-type calcium channels. Evidence for alternative splicing of the transcripts of three non-allelic genes," *Journal of Biological Chemistry*, vol. 265, no. 33, pp. 20430–20436, 1990.
- [32] UniProtKB/Swiss-Prot, 2013, <http://www.uniprot.org/uniprot/Q13936>.
- [33] L. Yu, C. Sun, D. Song et al., "Nuclear magnetic resonance structural studies of a potassium channel-charybdotoxin complex," *Biochemistry*, vol. 44, no. 48, pp. 15834–15841, 2005.
- [34] B. S. Zhorov, E. V. Folkman, and V. S. Ananthanarayanan, "Homology model of dihydropyridine receptor: implications for L-type Ca²⁺ channel modulation by agonists and antagonists," *Archives of Biochemistry and Biophysics*, vol. 393, no. 1, pp. 22–41, 2001.
- [35] A. Sali, L. Potterton, F. Yuan, H. Van Vlijmen, and M. Karplus, "Evaluation of comparative protein modeling by MODELLER," *Proteins*, vol. 23, no. 3, pp. 318–326, 1995.
- [36] M.-Y. Shen and A. Sali, "Statistical potential for assessment and prediction of protein structures," *Protein Science*, vol. 15, no. 11, pp. 2507–2524, 2006.

- [37] V. Z. Spassov, L. Yan, and P. K. Flook, "The dominant role of side-chain backbone interactions in structural realization of amino acid code. ChiRotor: a side-chain prediction algorithm based on side-chain backbone interactions," *Protein Science*, vol. 16, no. 3, pp. 494–506, 2007.
- [38] V. Z. Spassov, P. K. Flook, and L. Yan, "LOOPER: a molecular mechanics-based algorithm for protein loop prediction," *Protein Engineering, Design and Selection*, vol. 21, no. 2, pp. 91–100, 2008.
- [39] V. Z. Spassov and Y. A. N. Lisa, "A fast and accurate computational approach to protein ionization," *Protein Science*, vol. 17, no. 11, pp. 1955–1970, 2008.
- [40] Y. Jiang, A. Lee, J. Chen et al., "X-ray structure of a voltage-dependent K^+ channel," *Nature*, vol. 423, no. 6935, pp. 33–41, 2003.
- [41] S. B. Long, E. B. Campbell, and R. MacKinnon, "Crystal structure of a mammalian voltage-dependent Shaker family K^+ channel," *Science*, vol. 309, no. 5736, pp. 897–903, 2005.
- [42] G. M. Lipkind and H. A. Fozzard, "KcsA crystal structure as framework for a molecular model of the Na^+ channel pore," *Biochemistry*, vol. 39, no. 28, pp. 8161–8170, 2000.
- [43] I. Huber, E. Wappl, A. Herzog et al., "Conserved Ca^{2+} -antagonist-binding properties and putative folding structure of a recombinant high-affinity dihydropyridine-binding domain," *Biochemical Journal*, vol. 347, no. 3, pp. 829–836, 2000.
- [44] F. Corpet, "Multiple sequence alignment with hierarchical clustering," *Nucleic Acids Research*, vol. 16, no. 22, pp. 10881–10890, 1988.
- [45] S. C. Lovell, I. W. Davis, W. B. Arendall III et al., "Structure validation by $C\alpha$ geometry: ϕ, ψ and $C\beta$ deviation," *Proteins*, vol. 50, no. 3, pp. 437–450, 2003.
- [46] C. Colovos and T. O. Yeates, "Verification of protein structures: patterns of nonbonded atomic interactions," *Protein Science*, vol. 2, no. 9, pp. 1511–1519, 1993.
- [47] V. B. Chen, W. B. Arendall III, J. J. Headd et al., "MolProbity: all-atom structure validation for macromolecular crystallography," *Acta Crystallographica D*, vol. 66, no. 1, pp. 12–21, 2010.
- [48] I. W. Davis, L. W. Murray, J. S. Richardson, and D. C. Richardson, "MolProbity: structure validation and all-atom contact analysis for nucleic acids and their complexes," *Nucleic Acids Research*, vol. 32, pp. W615–W619, 2004.
- [49] I. W. Davis, A. Leaver-Fay, V. B. Chen et al., "MolProbity: all-atom contacts and structure validation for proteins and nucleic acids," *Nucleic Acids Research*, vol. 35, pp. W375–383, 2007.
- [50] M. J. Sippl, "Recognition of errors in three-dimensional structures of proteins," *Proteins*, vol. 17, no. 4, pp. 355–362, 1993.
- [51] M. Wiederstein and M. J. Sippl, "ProSA-web: interactive web service for the recognition of errors in three-dimensional structures of proteins," *Nucleic Acids Research*, vol. 35, pp. W407–410, 2007.
- [52] R. Lüthy, J. U. Bowie, and D. Eisenberg, "Assesment of protein models with three-dimensional profiles," *Nature*, vol. 356, no. 6364, pp. 83–85, 1992.
- [53] A. Bhattacharya, Z. Wunderlich, D. Monleon, R. Tejero, and G. T. Montelione, "Assessing model accuracy using the homology modeling automatically (HOMA) software," *Proteins*, vol. 70, no. 1, pp. 105–118, 2008.
- [54] O. Llorca, M. Betti, J. M. González, A. Valencia, A. J. Márquez, and J. M. Valpuesta, "The three-dimensional structure of an eukaryotic glutamine synthetase: functional implications of its oligomeric structure," *Journal of Structural Biology*, vol. 156, no. 3, pp. 469–479, 2006.
- [55] K. Teilum, J. C. Hoch, V. Goffin, S. Kinet, J. A. Martial, and B. B. Kragelund, "Solution structure of human prolactin," *Journal of Molecular Biology*, vol. 351, no. 4, pp. 810–823, 2005.
- [56] K. Ginalski, "Comparative modeling for protein structure prediction," *Current Opinion in Structural Biology*, vol. 16, no. 2, pp. 172–177, 2006.
- [57] D. Petrey and B. Honig, "Protein structure prediction: inroads to biology," *Molecular Cell*, vol. 20, no. 6, pp. 811–819, 2005.
- [58] M. K. Beissenhirtz, F. W. Scheller, M. S. Viezzoli, and F. Lisdat, "Engineered superoxide dismutase monomers for superoxide biosensor applications," *Analytical Chemistry*, vol. 78, no. 3, pp. 928–935, 2006.
- [59] J. Mansfeld, S. Gebauer, K. Dathe, and R. Ulbrich-Hofmann, "Secretory phospholipase A2 from *Arabidopsis thaliana*: insights into the three-dimensional structure and the amino acids involved in catalysis," *Biochemistry*, vol. 45, no. 18, pp. 5687–5694, 2006.
- [60] R. A. Engh and R. Huber, "Structure quality and target parameters," in *International Tables for Crystallography Volume F: Crystallography of Biological Macromolecules*, M. G. Rossmann and E. Arnold, Eds., pp. 382–392, Kluwer Academic Publishers, Dordrecht, The Netherlands, 2001.
- [61] B. Z. Peterson and W. A. Catterall, "Calcium binding in the pore of L-type calcium channels modulates high affinity dihydropyridine binding," *Journal of Biological Chemistry*, vol. 270, no. 31, pp. 18201–18204, 1995.
- [62] N. Pedemonte, D. Boido, O. Moran et al., "Structure-activity relationship of 1,4-dihydropyridines as potentiators of the cystic fibrosis transmembrane conductance regulator chloride channel," *Molecular Pharmacology*, vol. 72, no. 1, pp. 197–207, 2007.
- [63] C. O. Kappe, "4-Aryldihydropyrimidines via the Biginelli condensation: aza-analogs of nifedipine-type calcium channel modulators," *Molecules*, vol. 3, no. 1, pp. 1–9, 1998.
- [64] H. Ito, N. Klugbauer, and F. Hofmann, "Transfer of the high affinity dihydropyridine sensitivity from L-type to non-L-type calcium channel," *Molecular Pharmacology*, vol. 52, no. 4, pp. 735–740, 1997.
- [65] T. F. El-Moselhy, "QSAR and docking studies of 1,4-dihydropyridine calcium antagonists with methylsulfonylimidazolyl substituent based on genetic function approximation," *Chemistry and Biology Interface*, vol. 2, pp. 172–182, 2012.
- [66] R. Miri, K. Javidnia, H. Sarkarzadeh, and B. Hemmateenejad, "Synthesis, study of 3D structures, and pharmacological activities of lipophilic nitroimidazolyl-1,4-dihydropyridines as calcium channel antagonist," *Bioorganic and Medicinal Chemistry*, vol. 14, no. 14, pp. 4842–4849, 2006.
- [67] W. G. Nayler, "Amlodipine an overview," *Clinical Drug Investigation*, vol. 13, no. 1, pp. 1–11, 1997.
- [68] T. F. El-Moselhy, "Lipophilic 4-imidazolyl-1,4-dihydropyridines: synthesis, calcium channel antagonist activity and docking study," *Chemistry and Biology Interface*, vol. 3, pp. 123–136, 2013.
- [69] A. Foroumadi, N. Analuie, M. Rezvanipour et al., "Synthesis and calcium channel antagonist activity of nifedipine analogues with methylthioimidazole substituent," *Farmaco*, vol. 57, no. 3, pp. 195–199, 2002.
- [70] M. Hosseini, R. Miri, M. Amini et al., "Synthesis, QSAR and calcium channel antagonist activity of new 1,4-dihydropyridine derivatives containing 1-methyl 1,4,5-dichloroimidazolyl substituents," *Archiv der Pharmazie*, vol. 340, no. 10, pp. 549–556, 2007.

- [71] A. Shafiee, A. R. Dehpour, F. Hadizadeh, and M. Azimi, "Syntheses and calcium channel antagonist activity of nifedipine analogue with methylsulfonylimidazolyl substituent," *Pharmaceutica Acta Helvetiae*, vol. 73, no. 2, pp. 75–79, 1998.
- [72] A. Zarghi, H. Sadeghi, A. Fassihi, M. Faizi, and A. Shafiee, "Synthesis and calcium antagonist activity of 1,4-dihydropyridines containing phenylaminoimidazolyl substituents," *Farmaco*, vol. 58, no. 11, pp. 1077–1081, 2003.
- [73] A. Senatore, A. N. Boone, S. Lam, T. F. Dawson, B. S. Zhorov, and J. D. Spafford, "Mapping of dihydropyridine binding residues in a less sensitive invertebrate L-type calcium channel (LCav1)," *Channels*, vol. 5, no. 2, pp. 173–187, 2011.
- [74] J. Tamargo, J. López-Sendón, E. Delpon, M. González-Morales, and E. de Miguel, "Cardiovascular effects of the new dihydropyridine derivative elgodipine," *Arzneimittel-Forschung*, vol. 41, no. 9, pp. 895–900, 1991.
- [75] N. Daryabari, T. Akbarzadeh, M. Amini, R. Miri, H. Mirkhani, and A. Shafiee, "Synthesis and calcium channel antagonist activities of new derivatives of dialkyl 1,4-dihydro-2,6-dimethyl-4-(5-phenylisoxazol-3-yl)pyridine-3,5-dicarboxylates," *Journal of the Iranian Chemical Society*, vol. 4, no. 1, pp. 30–36, 2007.
- [76] A. Shafiee, A.-R. Dehpour, F. Hadizadeh, and B. Rezaei, "Synthesis and calcium channel antagonist activity of nifedipine analogues with chloroindolyl substituent," *DARU Journal of Pharmaceutical Sciences*, vol. 8, no. 3-4, pp. 32–36, 2000.
- [77] T. F. El-Moselhy, "Synthesis of 1, 4-Dihydropyridine Hantzsch Ester as potential calcium channel blockers," *Alexandria Journal of Pharmaceutical Sciences*, vol. 16, pp. 35–39, 2002.
- [78] K. Kuroda, Y. Fukuda, K. Nakao, and T. Inukai, "Effects of felodipine on vascular smooth muscle in comparison with nifedipine," *Arzneimittel-Forschung*, vol. 41, no. 7, pp. 709–714, 1991.
- [79] D. Hadjipavlou-Litina, "Calcium ion channels and their blockers," in *Ion Channels and Their Inhibitors*, S. P. Gupta, Ed., pp. 265–288, Springer, New York, NY, USA, 2011.



Hindawi

Submit your manuscripts at
<http://www.hindawi.com>

